Size-Dependent Optical Nonlinearity of Au Nanocrystals

**R. Sreeja,[a,*] P. M. Aneesh,[a,*] Arun Aravind,[a,*] R. Reshmi,[a,*] Reji Philip,[b]
and M. K. Jayaraj[a,**,z]**

[a]*Optoelectronic Devices Laboratory, Department of Physics, Cochin University of Science and Technology,
Kochi, Kerala 682 022, India*
[b]*Light and Matter Physics Group, Raman Research Institute, Bangalore, Karnataka 560 080, India*

Gold nanoparticles of different sizes are prepared by laser ablation of the gold target in deionized water. The UV/visible absorption spectra show surface plasmon resonance bands that are redshifted in wavelength with an increase in particle size. An increase in particle size is observed with increasing laser pulse energy. The optical absorptive nonlinearity of the nanoclusters shows an optical-limiting-type nonlinearity, which finds application in the fabrication of optical-limiting devices. The limiting efficiency decreases with an increase in particle size. The Au nanoparticle shows good nonlinear refraction, which is of a self-defocusing nature. Both the real and imaginary parts of nonlinear susceptibility increase with a decrease in particle size. A stable nonlinear device is fabricated by incorporating Au nanocrystals in a polymer matrix.
© 2009 The Electrochemical Society. [DOI: 10.1149/1.3184188] All rights reserved.

Metal nanoparticles occupy a marvelous field of research interest due to their remarkable properties of Mie resonances[1] and quantum size effects[2] in nonlinear optics. Nanoparticle metal-colloidal solutions of the noble metals of copper, silver, and gold exhibit a very intense color, which is absent in the bulk materials as well as in the individual atoms. This coloration is due to the collective oscillation of the free conduction electrons induced by the interacting electromagnetic fields.[3-6] These resonances are called surface plasmon resonances (SPRs). Due to these properties, they are selected as prominent materials for a wide range of applications, including nonlinear optical devices, data storage, telecommunication, biosensors, etc. Gold-nanoparticle-based DNA detection is reported earlier.[7] Nanocomposites of gold–silica for the detection of human ovarian cancer cells are also reported.[8] The Mie theory and the Maxwell–Garnett theory[9] explain the SPR band in terms of higher moment oscillations and particle size.[10] It is proved that the electrical and optical properties are strongly dependent on the size and shape of the nanoparticles.[11] A simulation based on quasi-static, scattering, and local field theory has been developed to describe the optical properties of gold nanospheres. Numerical calculations show that both the intensity and the wavelength maximum of the absorption, light scattering, and fluorescence emission are sensitive to the dielectric constant of the surrounding medium.[12] Several methods have been proposed to control the size and shape of nanoclusters, including chemical reduction, photolysis of gold salts, and ultrasonic reduction. However, these chemical reduction methods[13-15] produce by-products that contaminate and affect the stability of the clusters. In this situation, the safe and practically simple methods, such as laser ablation of solid targets, have been introduced.[16] Nano- and femtosecond pulsed laser ablations of gold nanoclusters are reported in various solvents such as water, ethanol, and toluene.[16-18] The resulting solution consists of only the colloids and the solvent; no by-products of gold are present. In this paper, we report nanosecond ablation of gold in deionized water, and the dependence of laser fluence and ablation time on the optical properties of the clusters are analyzed. The nonlinear optical properties, such as nonlinear refraction and nonlinear absorption, are also studied using the single-beam Z-scan technique.[19]

Nanoparticles have been suggested for applications in nonlinear optics for the past decade due to the enhanced third-order susceptibility of metal nanoclusters and metal nanocomposites.[20-23] The large optical nonlinearity near the SPR can be explained on the basis of local field enhancement inside the particle.[24,25] The optical nonlinearity of glass-embedded silver nanoclusters under ultrafast laser excitation has been reported earlier, where the silver nanoclusters are ion exchanged into the soda-lime silicate glass, and external annealing at a higher temperature is required to tune the cluster size.[24] Compared to these ion-exchange methods, the laser ablation is at room temperature and is a relatively easier method where nanoparticle size tunability is well controlled. Gold nanoparticles have the additional advantage that they are nonreactive and nonoxidizable. Aqueous metal nanocolloids may undergo a partial sedimentation, and this may affect the stability of optical nonlinearity.[26] In a device point of view, these metal nanocrystals can be embedded in a suitable dielectric host matrix so as to achieve better stability compared to a colloidal solution. If the dielectric matrix used offers ease of flexibility, it is an additional advantage in the device point of view. Hence, a polymer matrix does better compared to any other dielectric media such as silica and TiO_2.[27] In the present paper, the gold nanoparticles showing better nonlinearity are embedded in a stable polymer matrix so as to yield ease of flexibility as well as long-term stability in a device point of view as compared to the metal nanocolloids. The optical nonlinearity of polymer-embedded Au nanocrystals is analyzed using the single-beam Z-scan technique.

Experimental

The second harmonics of a Nd:yttrium aluminum garnet (Nd:YAG) laser (532 nm) operating at a repetition rate of 10 Hz was focused onto a high purity gold target immersed in 15 mL of deionized water. Keeping the ablation time the same (1 h), the laser fluence was varied from 1.2 to 3.8 J/cm². The UV/visible absorption spectra of the as-prepared nanocluster solutions were recorded using a JASCO500 spectrophotometer in the wavelength region of 350–800 nm. The sizes of the nanoparticles were analyzed by transmission electron microscopy (TEM). Poly vinyl alcohol (PVA) (2 g) was mixed with a 20 mL water solution and stirred for 1 h at a temperature of 50°C. To this viscous fluid, 15 mL of Au/water solution was added dropwise and again stirred for 2 h at room temperature. For a thorough mixing of Au nanocrystals in the PVA matrix, the resultant viscous colloidal solution was subjected to ultrasonic agitation for 15 min. Soon after the agitation, 3 mL of the Au/PVA solution was spin coated on a glass plate at 1000 rpm so as to get a thin uniform film with a thickness of 1 μm in which Au nanocrystals were embedded inside the dielectric host matrix.

The nonlinear optical properties were analyzed using the single-beam Z-scan technique. The experimental setup for the nonlinear study is shown in Fig. 1. The experimental setup consisted of a Nd:YAG laser, which functioned as the laser source, working at 532 nm and operating at a repetition rate of 10 Hz. The incident beam was split into two; one part was taken as the reference beam, and the other beam was allowed to transmit through the sample. The laser beam was focused onto the sample using a lens with a focal length
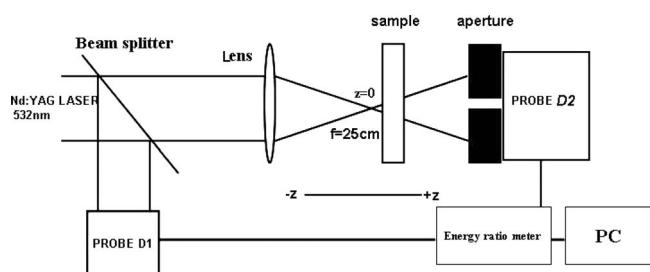
Figure 1. Schematic of closed aperture Z-scan setup.

of 25 cm. The sample was translated in the spatially varying intensity region on either side ($-z$ to $+z$) of the focal point ($z = 0$) using the translation stage of an automated stepper motor. The reference laser fluence, the transmitted fluence. and the ratio between them were measured using probes D1 and D2 of an automated energy ratio meter (RJ-7620 energy ratio meter) simultaneously for different positions of z. The dependence of the incident laser fluence on the nonlinear absorption and the nonlinear refraction was analyzed using open (without aperture) and closed aperture (with aperture) Z-scan techniques, respectively.

Results and Discussion

The mechanism of the nanoparticle growth during liquid-phase pulsed laser ablation can be explained using the model presented by Mafune et al.[28] According to this model, while the plume expands in a media such as water, small polar molecules of water create an electrical bilayer around the nanoparticles.[29] In these solvents, the OH group on the gold nanoparticles generated a surface charge, and an electrical bilayer was formed. The electrostatic repulsion between the gold nanoparticles prevented further growth and resulted in stable clusters.

In gold nanoparticles with a size range of 2–99 nm, it is expected that the position of the maximum optical absorption appear between 520 and 580 nm.[30] Figure 2 shows the absorption spectra obtained in the samples prepared at different laser fluences varying from 1.2 to 3.8 J/cm². The UV/visible absorption spectra of the samples showed strong surface plasmon peaks only in the visible region (518–530 nm), a property shown by spherical Au nanoparticles as proposed by the Mie theory. For nonspherical particles such as nanorods, there were additional plasmon modes at a higher wavelength (800 nm) corresponding to the longitudinal mode of oscillation and the transverse mode of oscillation (around 520 nm) of the free elec-
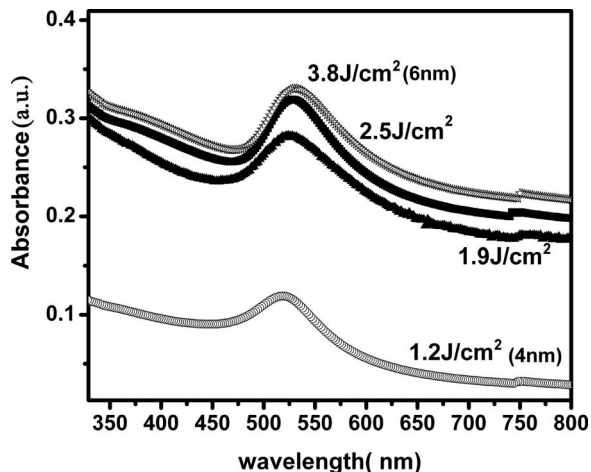
tron cloud.[31] The presence of a single plasmon peak in the lower wavelength proposed a spherical shape of the Au nanocrystals. A redshift in the absorption maxima from 518 to 530 nm indicated an increase in particle size.[24] When the size of the particle increases, light cannot polarize the nanoparticle homogenously because in larger clusters, the localization of the d band electrons increased the screening of the ions by surface electrons, reducing the polarizability near the surface, and the retardation effect led to the excitation of higher order modes.[31] This was regarded as an extrinsic size effect. This led to a redshift in the SPR peak with an increase in nanoparticle size.

The amplitude of the SPR peak increased with an increase in the ablation fluence, which was attributed to the increase in the number of gold nanoparticles in water. The broadening of the absorption band with a decrease in particle size was observed, which was attributed to the increased damping known as Landau damping.[8] As long as the particles were apart, there was no contribution to the observed broadening, but when the volume fraction of the Au nanoparticles increased, an interparticle interaction came into play.

The dependence of the absorption cross section of the plasmon resonance on the particle size and the surrounding dielectric media, as proposed by the Drude model for the spherical metal nanoparticle, can be used in the simulation so as to find out the particle size. The model consisted of a sphere of radius R in a suspending medium. The nanosphere had a dielectric function ε_1, and the embedding medium had a dielectric function ε_2. $\varepsilon_1 = \varepsilon_{1r} + i\varepsilon_{1i}$ can have real and imaginary frequency-dependent components. In the Drude model, the frequency-dependent complex dielectric constant can then be written as[32]

$$\varepsilon(\omega) = \varepsilon_r + i\varepsilon_i = \varepsilon_b(\omega) - \frac{\dfrac{\omega_p^2}{\omega^2}}{1 + \dfrac{1}{\omega^2\tau^2}} + i\frac{\dfrac{\omega_p^2}{\omega^2}}{\omega\tau\left(1 + \dfrac{1}{\omega^2\tau^2}\right)} \quad [1]$$

where $\varepsilon_b(\omega)$ is the dielectric function of the bulk metal, which is due to the interband transition, ω_p denotes the plasmon frequency of the bulk metal, τ is the relaxation time, and ω is the frequency of the electromagnetic wave. The absorption cross section is given as follows

$$\sigma_{abs} = \frac{24\pi^2 R^3 \varepsilon_{1i}\varepsilon_2}{\lambda[(\varepsilon_{1r} + 2\varepsilon_2)^2 + \varepsilon_{1i}^2]} \quad [2]$$

The simulation and the experimental plots obtained for the nanoparticles prepared at laser fluences of 1.2 and 3.8 J/cm² are shown in Fig. 3a and b, respectively. The particle sizes calculated from the simulation analysis were 4 and 6 nm for the nanoparticles prepared at 1.2 and 3.8 J/cm² ablation fluences, respectively.

The TEM, high resolution transmission electron microscopy (HRTEM), selected area electron diffraction (SAED) patterns and size histograms of the nanoparticles prepared at 1.2 and 3.8 J/cm² are shown in Fig. 4. The TEM image shows the gold nanoparticles distributed uniformly in the aqueous media, confirming the spherical shape of the nanoparticles, as observed in the UV/visible absorption spectra. The average particle sizes of the Au nanoclusters were 4 and 6 nm for 1.2 and 3.8 J/cm², respectively. Those used in the present study were similar to the values obtained from simulating the absorption spectra. TEM analysis showed that an almost similar particle size (4 nm) can be created at a much lower laser fluence of 1.2 J/cm² as compared to the higher laser fluence of 60 J/cm², as reported by Kabashin and Meunier using the femtosecond laser ablation.[16] d values obtained from the SAED pattern matched well with the (220), (200), and (400) planes of gold. The HRTEM showed the atomic planes where the d spacing was 2.35 Å corresponding to the (111) plane of gold.

The Au nanocluster prepared in water at a fixed laser fluence of 1.9 J/cm² for different durations of 1, 2, and 3 h showed an SPR peak at the same position of 520 nm (Fig. 5). It was reported that the
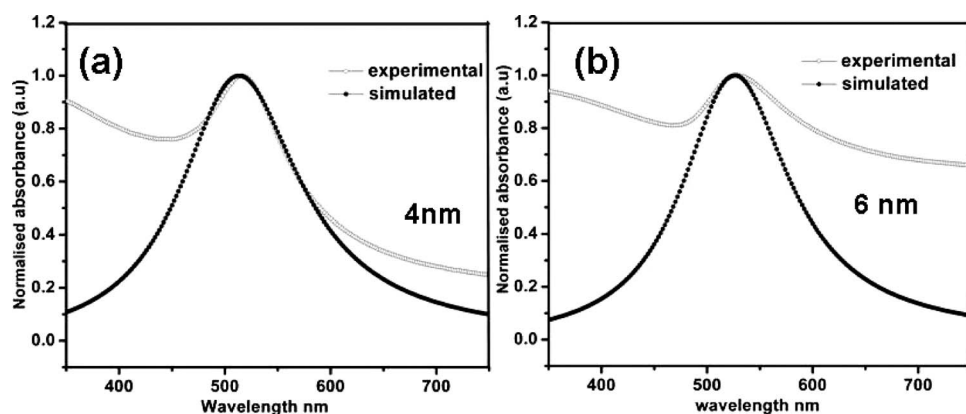

Figure 2. UV/visible absorption spectra of Au nanoclusters prepared at different laser fluences.

Figure 3. Experimental and simulated absorption spectra of nanoparticles with different sizes: (a) 4 and (b) 6 nm.

growth of nanoparticles with nanosecond lasers showed a reduction in particle size due to the efficient radiation absorption by the ablated particles.[17] No such reduction in particle size was observed in our study. Only an enhancement in the absorbance was observed in the UV/visible spectrum, which was due to the increased particle density of the samples with an increase in ablation duration. Therefore, the simulation of the absorption spectra indicated an almost constant size (4 nm) for the Au nanoparticles prepared at 1.9 J/cm^2 and independent of the ablation duration.

In the metal nanoparticles, the optical properties were due to the d and the outermost s–p conduction electrons. In band calculations, the outermost d and s electrons of the constituent atoms must be treated as leading to six bands. Five of them are fairly flat and lie a few electron volts below the Fermi level; they are usually denoted as d bands. The sixth one being an almost free electron is roughly parabolic, with an effective mass close to that of a free electron. This last band is called s–p band or conduction band. To induce a transition between the d bands and the conduction band, the photon energy $\hbar\omega$ has to be larger than a gap of energy $\hbar\omega_g$. In gold, this gap energy is 1.7 eV. These interband transitions explain the color of bulk gold. In metal colloids, there is one absorption band due to SPR; for gold, $\hbar\omega_s$ corresponds to 2.3 eV. Hence, near the SPR, both d electrons as well as the conduction electrons contribute to the nonlinear response. Also, there is a contribution from the saturation of the interband transitions. The conduction electron contribution as a whole is called intraband. The susceptibility induced by the intra-

band transitions is an electric dipole, and it is attributed to the confinement of the free electrons. It is, therefore, strongly particle size dependent, varying as a^{-3} when the particle size is $a \ll a_0$, where a_0 is a parameter related to the Fermi energy and the dephasing time of the conduction electrons.[12] In gold and for the 532 nm light, the value of a_0 is ~13.6 nm.

The optical absorptive nonlinearities were measured by the open aperture Z-scan technique. Optical limiters are those materials whose transmittance falls down with an increase in the incident laser fluence after a threshold value of the incident fluence, which is due to several phenomena such as free-carrier absorption, two-photon absorption, three-photon absorption, and nonlinear scattering. In nanoparticle systems, nonlinear scattering due to thermally induced nonlinearity is an alternative process that can mimic nonlinear absorption. Nonlinear scattering in gold nanoparticles has been reported earlier.[23] Heat transfer from the excited nanoparticles to the surrounding matrix is usually treated by the Fourier heat conduction theory.[33] However, in smaller particles where the particle size is much smaller than the heat carrier mean free path, only very few carrier-scattering events occur around the heated metal nanosphere.[24] Therefore, the nonlinearity aroused here is surely of multiphoton origin.

When excited at 532 nm (2.33 eV), the electrons in the filled d band of gold were excited to the unoccupied states in the conduction band due to interband transitions. These excited electrons are free carriers possessing a whole spectra of kinetic as well as potential
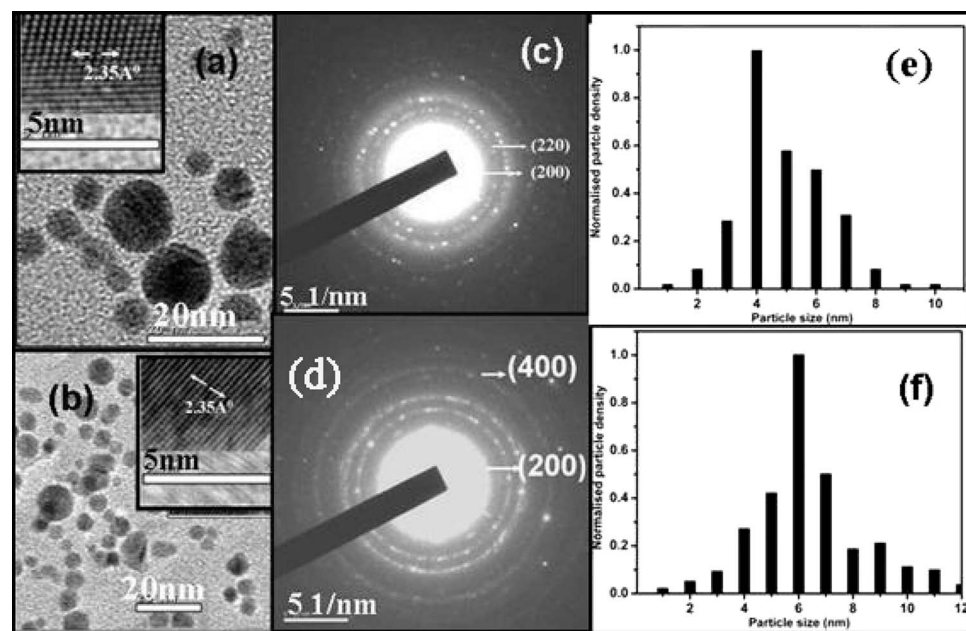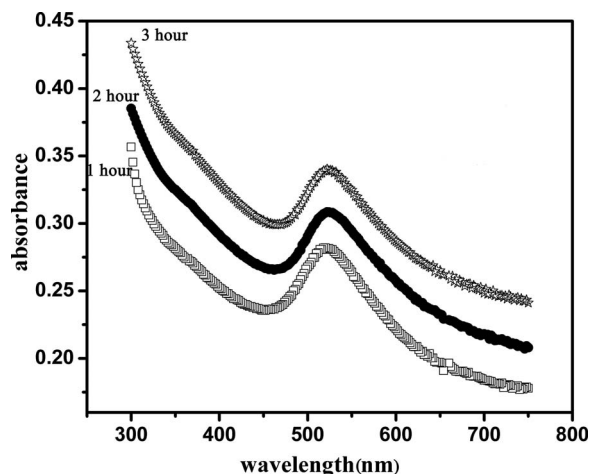

Figure 4. [(a) and (b)] TEM, [inset of (a) and (b)] HRTEM, [(c) and (d)] SAED patterns, and [(e) and (f)] size histograms of Au nanoclusters prepared at 1.2 (top row) and 3.8 J/cm^2 (bottom row).

Figure 5. UV/visible absorption spectra of Au nanoclusters prepared at a laser fluence of 1.9 J/cm^2 for different durations.

energies, which may lead to transient absorption due to free carrier absorption. A part of the excited electrons were pumped to even higher energy levels, causing excited state absorption. Thus, the origin of the reverse saturable absorption in gold nanoparticles was attributed to the excitations from the plasmon band to the free carrier band. Also, there was a chance of a bleach or a reduction in the intensity of the ground-state plasmon band that was almost synchronous with the primary photon absorption at a resonant excitation.[34] The experimentally obtained curve in the present study (Fig. 6) was of an optical-limiting type where the transmittance falls down with an increasing incident laser fluence.

Experimental data fit well with the theoretical equation (Eq. 3) for normalized transmittance $T(z, S = 1)$ corresponding to the nonlinear absorption[19]

$$T(z, S = 1) = 1/\sqrt{\pi} q_0(z,0) \int \ln[1 + q_0(z,0)e^{-\tau^2}]d\tau \qquad [3]$$

where $q_0(z,0) = \beta I_0 L_{\mathrm{eff}}$, where β is the nonlinear absorption coefficient, L_{eff} is given by $(1 - e^{-\alpha L})/\alpha$ (L is the sample length and α is the linear absorption coefficient), and I_0 is the incident intensity. The experimental data points are fitted with the theoretical equation (Eq. 3), with β taken as the fitting parameter, and the value of β corre-
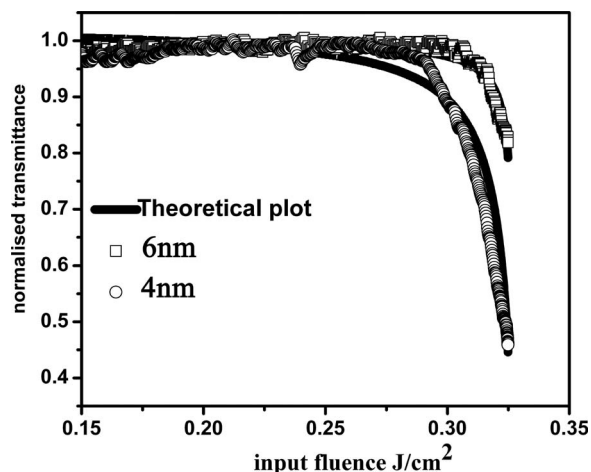
Figure 6. Optical-limiting characteristic of the Au nanoclusters of 4 and 6 nm in water. The solid line represents theoretical fitting to the experimental data.

sponding to the best theoretical fit is taken. The solid line in Fig. 6 represents the theoretical fitting to the experimentally obtained data points.

The optical absorptive nonlinearities of the samples prepared at the lowest (1.2 J/cm^2) and the highest (3.8 J/cm^2) laser ablation energy showed that a better absorptive nonlinearity was obtained for the smallest nanoparticles (4 nm). The nonlinear absorption coefficients β corresponding to 4 and 6 nm were 4.737×10^{-10} and 4.37×10^{-11} m/W, respectively, i.e., a decrease in the value of β with an increase in the size of the nanoparticles. The nonlinear absorption was reduced with an increase in the particle size, which was due to the excitation wavelength close to the SPR frequency.[35] From the SPR peak position of the clusters, we can see that the chance of a band bleach was least for the smallest nanoparticles, whereas it was higher for the larger nanoparticles. So, as the particle size increased, the dip in the optical-limiting curve decreased (the limiting efficiency decreased), which was due to the partial bleaching of the ground-state plasmon band for the larger size nanoparticles at 532 nm.[24] The $\mathrm{Im}(\chi^{(3)}), \chi_I(3)$ is related to the nonlinear absorption coefficient β through the following equation

$$\chi_I(3) = (n_0^2 \lambda c \beta)/48\pi^3 \qquad [4]$$

where λ and c are the wavelengths of the incident laser beam (532 nm) and the velocity of light in vacuum, respectively. The value of $\mathrm{Im}(\chi^{(3)})$ was calculated to be 0.757×10^{-10} and 0.698×10^{-10} esu for the 4 and 6 nm Au nanoparticles, respectively. Hence, these Au nanoclusters are valuable applications for optical-limiting device fabrications.

The Au nanoclusters in water showed a good nonlinear refraction, which was attributed to the self-defocusing effect in the sample. The excited hot electrons (electrons with higher energy than Fermi energy) were thermalized by dissipating the excess energy through scattering processes.[36] The excess thermal energy increased the surrounding temperature and generated a temperature gradient. This temperature gradient led to a variation in the refractive index, which is called a thermal lens.[37] In addition to the thermal lens, the population redistribution between the excited and the ground-state conduction bands also played an important part in the variation in the refractive index called a population lens.[38]

The closed aperture data contained both the effects of nonlinear absorption as well as the refraction. Therefore, the closed aperture Z-scan traces of the Au nanoclusters were divided with the open aperture traces to eliminate the effect of nonlinear absorption. The closed aperture transmittance $T(z, \Delta\phi_0)$ is related to the on-axis phase shift at the focus $\Delta\phi_0$ by[19]

$$T(z, \Delta\phi_0) \approx \left[1 + \frac{4\Delta\phi_0 x}{(x^2 + 9)(x^2 + 1)} \right] \qquad [5]$$

where

$$x = (z/z_0)$$

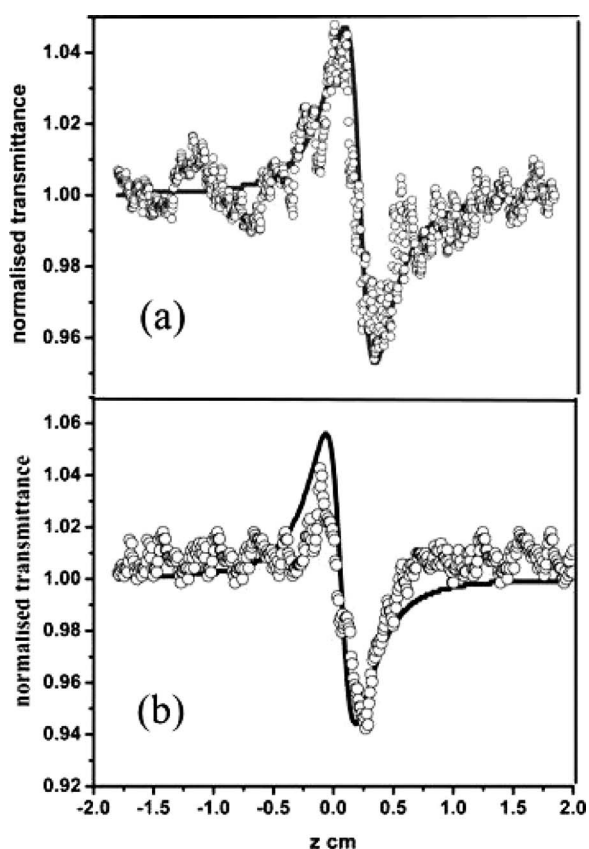and $\Delta\phi_0$ is related to the nonlinear refractive index γ through

$$\gamma = \frac{\lambda \Delta\phi_0}{2L_{\mathrm{eff}} I_0} \qquad [6]$$

Therefore, fitting the closed aperture data with the theoretical equation (Eq. 5), where γ, is taken as the fitting parameter, yields the value of the nonlinear refractive index γ. The nonlinear refractive index γ and the real part of the third-order optical nonlinear susceptibility $\mathrm{Re}(\chi^{(3)})$ can be given by Eq. 7

$$\mathrm{Re}(\chi^{(3)}) = 2n_0^2 c\gamma\varepsilon_0 \qquad [7]$$

where n_0 is the linear refractive index of the sample, ε_0 is the permittivity of free space, and c is the velocity of light in vacuum.

The typical closed aperture curves for the Au nanoclusters of 4 and 6 nm are shown in Fig. 7a and b, respectively. The values of the nonlinear refractive index γ are -2.421×10^{-15} and -1.115
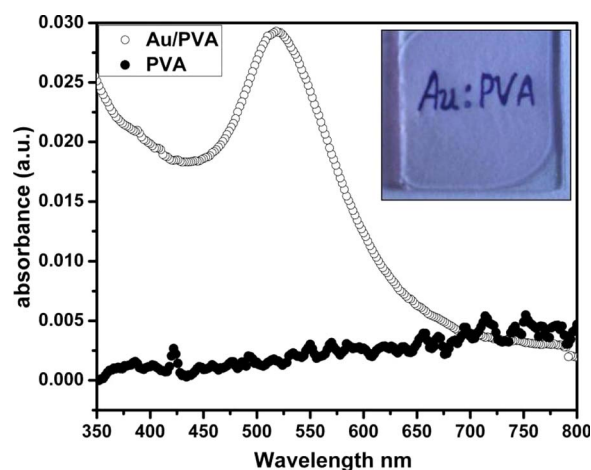
Figure 7. Closed aperture Z-scan traces of the Au nanoclusters of sizes (a) 6 and (b) 4 nm.

Figure 8. (Color online) UV/visible absorption spectra of Au/PVA films (inset shows the photo of Au/PVA film).

$\times 10^{-15}$ m^2/W, for the nanoparticles of 4 and 6 nm, respectively. The Re($\chi^{(3)}$) were calculated to be -38.37×10^{-10} and -4.07×10^{-10} esu for the 4 and 6 nm nanoparticles, respectively. The enhancement in the Re($\chi^{(3)}$) of the lower sized nanoparticles originated from the size-dependent enhancement in the local electric field inside the nanoparticle. The enhancement of the oscillator strength per nanoparticles was by a factor of a^{-3}, where a is the diameter of the nanoparticle.[12] The size dependence in the real part nonlinear susceptibility Re($\chi^{(3)}$) indicated the contribution from the intraband transitions in the conduction band.

For nonlinear optical applications, it is better to incorporate the nanoparticles immobilized in a suitable matrix such as polymer or glass. The ease of flexibility that the polymer matrix provides as compared to a rigid fragile matrix such as glass makes it best to incorporate Au nanoparticles in the polymer matrix for fabricating devices. Lower sized (4 nm) nanoparticles having high values of γ as well as β are embedded inside the PVA matrix so as to achieve a stable optical-limiting device. The UV/visible absorption spectra of the Au/PVA film as well as pure PVA film are depicted in Fig. 8, which shows the presence of strong SPR bands peaked at 520 nm in Au/PVA, indicating the incorporation of Au in the matrix. A slight shift (2 nm) in the SPR compared to the colloidal solution in water may be due to a change in the dielectric constant of the medium used. The inset of Fig. 8 shows the photograph of the Au/PVA thin film with the writing beneath it.

The open as well as closed aperture Z-scan traces of the Au/PVA film were taken using the Z-scan technique. Figure 9a shows the optical-limiting curve of the Au/PVA films, whereas Fig. 9b gives the closed aperture curve showing the negative refractive index-type nonlinearity. The values of β and γ are 4.16×10^{-9} and -2.8×10^{-14} m^2/W, respectively. This means that the optical limiting as well as the nonlinear refraction of the Au nanocrystals in the poly-

mer film were better compared to the Au/water colloidal solution. The enhancement in the nonlinear absorption was attributed to the increased density and stability of the Au nanocrystals in the polymer matrix as compared to that in the water media. The nonlinear refraction may contain electronic as well as thermal contributions. However, the enhancement in the refractive index may be attributed to the thermally induced lensing in the Au/PVA as compared to the Au/water colloidal solution. The excited hot electrons were thermalized by dissipating the excess heat energy through the scattering process.[36] The excess thermal energy increased the surrounding temperature and generated a temperature gradient, dS/dT. This temperature gradient led to a variation in the refractive index (dS/dT), which is called a thermal lens.[37] Phase shift (θ) is suffered by the incident laser beam as a result of thermal lensing

$$\theta \alpha dS/dT$$

For liquid samples, $dS/dT = dn/dT$, whereas in solid samples, dS/dT involves contribution from dn/dT, end-phase curvature, and thermal stress.[38] Larger expansion of the hotter center compared to the cooler edge of the solid sample led to an end-face curvature contribution, and the cooler part of the sample prevented the expansion of its hotter center from generating thermal stress. Hence, the induced phase shift in a solid sample was higher as compared to a liquid sample. This may be the reason for the enhanced nonlinear refractive index in the thin film sample. However, a detailed analysis may be required to completely determine the exact phenomena behind the high value of the nonlinear refraction shown by the Au nanocrystals in the polymer matrix.

The values of the nonlinear absorption coefficient as well as the refractive index were comparatively better compared to those reported earlier in the Au colloids as well as the Au thin films.[39-41] Therefore, the optical-limiting efficiency as well as the self-defocusing nature are much better compared to earlier reports. Hence, the Au/PVA films are a valuable material for nonlinear applications involving optical limiting and self-defocusing. The Au nanocrystals were very stable inside the polymer matrix and worked efficiently for long-term applications.

Conclusion

Gold nanoparticles of different sizes were produced by laser ablation of a gold target in deionized water. An increase in the particle size was observed with increasing laser pulse energy. The absorption spectrum was redshifted in wavelength with an increase in the particle size. The optical absorptive nonlinearity of the nanoclusters showed an optical-limiting-type nonlinearity, which finds application in the fabrication of optical-limiting devices. The efficiency of limiting increased with a decrease in the particle size. The nonlinear
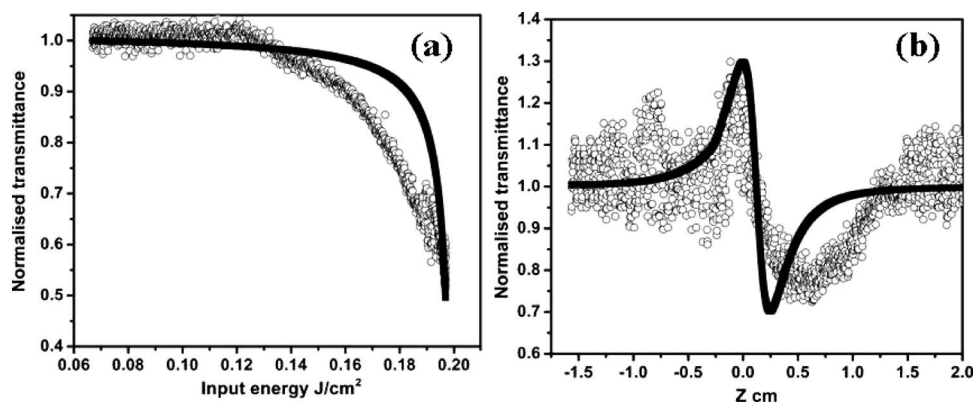
Figure 9. (a) The optical-limiting and (b) self-defocusing curves of Au nanocrystals in PVA matrix.

refraction of the Au nanoclusters showed a negative index value, indicating self-defocusing-type nonlinearity. Both the real and imaginary parts of nonlinear susceptibility increased with a decrease in the particle size, which was attributed to the size-dependent enhancement in the oscillator strength of the nanoparticle. The stable and flexible nonlinear devices were fabricated by incorporating the Au nanocrystals showing better nonlinearity in a PVA matrix. The enhancement in the nonlinear refractive index for the Au nanocrystals in the polymer matrix as compared to the Au nanocrystals in water was attributed to the thermal effects arising in the solid film.

Acknowledgments

References

1. M. Kerker, *The Scattering of Light and Other Electromagnetic Radiation*, p. 54, Academic, New York (1969).
2. U. Kreibig and M. Vollmer, *Optical Properties of Metal Clusters*, p. 14, Springer-Verlag, New York (1995).
3. A. Cottey, *J. Phys. C*, **4**, 1734 (1971).
4. G. C. Papavassiliou, *Prog. Solid State Chem.*, **12**, 185 (1979).
5. B. S. Yilbas, R. Davies, Z. Yilbas, and A. Koc, *Pramana*, **34**, 473 (1990).
6. C. F. Bohren and D. R. Huffman, *Absorption and Scattering of Light by Small Particles*, p. 524, John Wiley & Sons, New York (1983).
7. G. Festag, A. Steinbruck, A. Wolff, A. Csaki, R. Moller, and W. Fritzsche, *J. Fluoresc.*, **15**, 161 (2005).
8. Y. K. Mishra, S. Mohapatra, D. K. Avasthi, D. Kabiraj, N. P. Lalla, J. C. Pivin, H. Sharma, R. Kar, and N. Singh, *Nanotechnology*, **18**, 345606 (2007).
9. J. C. M. Garnett, *Philos. Trans. R. Soc. London*, **203**, 385 (1904).
10. Y. Xia and N. J. Halas, *MRS Bull.*, **30**, 338 (2005).
11. P. Mulvaney, *Langmuir*, **12**, 788 (1996).
12. F. Hache, D. Ricard, C. Flytzanis, and U. Kreibig, *Appl. Phys. A: Solids Surf.*, **47**, 347 (1988).
13. M. T. Reetz, M. Winter, and B. Tesche, *Chem. Commun. (Cambridge)*, **1997**, 147.
14. F. Favier, E. M. Walter, M. P. Zach, T. Benter, and R. M. Penner, *Science*, **293**, 2227 (2001).
15. J. Hu, T. W. Odom, and C. M. Lieber, *Acc. Chem. Res.*, **32**, 435 (1999).
16. A. V. Kabashin and M. Meunier, *J. Appl. Phys.*, **94**, 7941 (2003).
17. R. M. Tilaki, A. Irajizad, and S. M. Mahadevi, *Appl. Phys. A: Mater. Sci. Process.*, **84**, 215 (2006).
18. V. Amendola, G. A. Rizzi, S. Polizzi, and M. Meneghetti, *J. Phys. Chem. B*, **109**, 23125 (2005).
19. M. Sheik-Bahae, A. A. Said, and E. W. Van Stryland, *Opt. Lett.*, **14**, 955 (1989).
20. Y. Hamanaka, K. Fukuta, A. Nakamura, L. M. Liz-Marzan, and P. Mulvaney, *Appl. Phys. Lett.*, **84**, 4938 (2004).
21. M. Ballesteros, J. Solis, R. Serna, and C. N. Afonso, *Appl. Phys. Lett.*, **74**, 2791 (1999).
22. S. W. Lu, U. Sohling, M. Mennig, and H. Schmidt, *Nanotechnology*, **13**, 669 (2002).
23. L. Francois, M. Mostafavi, J. Belloni, J. F. Delouis, J. Delaire, and P. Feneyrou, *J. Phys. Chem. B*, **104**, 6133 (2000).
24. B. Karthikeyan, J. Thomas, and R. Philip, *Chem. Phys. Lett.*, **414**, 346 (2005).
25. N. Pinçon, B. Palpant, D. Prot, E. Charron, and S. Debrus, *Eur. Phys. J. D*, **19**, 395 (2002).
26. V. A. Karavanskii, A. V. Simakin, V. I. Krasovskii, and P. V. Ivanchenko, *Quantum Electron.*, **34**, 644 (2004).
27. N. Venkatram, R. S. S. Kumar, D. N. Rao, S. K. Medda, S. De, and G. De, *J. Nanosci. Nanotechnol.*, **6**, 1990 (2006).
28. F. Mafuné, J. Y. Kohno, Y. Takeda, T. Kondow, and H. Sawabe, *J. Phys. Chem. B*, **104**, 9111 (2000).
29. J. Turkevich, P. C. Stevenson, and J. Hillier, *Discuss. Faraday Soc.*, **11**, 55 (1951).
30. G. Fu, W. Cai, Y. Gan, and J. Jia, *Chem. Phys. Lett.*, **385**, 15 (2004).
31. S. Link and M. A. E. Sayed, *Annu. Rev. Phys. Chem.*, **54**, 331 (2003).
32. R. D. Averitt, D. Sarkar, and N. J. Halas, *Phys. Rev. Lett.*, **78**, 4217 (1997).
33. G. Chen, *J. Nanopart. Res.*, **2**, 199 (2000).
34. R. Philip, G. R. Kumar, N. Sandhyarani, and T. Pradeep, *Phys. Rev. B*, **62**, 13160 (2000).
35. P. P. Kiran, B. N. S. Bhaktha, and D. N. Rao, *J. Appl. Phys.*, **96**, 6717 (2004).
36. J. Y. Bigot, V. Halte, J. C. Merle, and A. Daunois, *Chem. Phys.*, **251**, 181 (2000).
37. J. P. Gordon, R. C. C. Leite, R. S. Moor, S. P. S. Porto, and J. R. Whinnery, *J. Appl. Phys.*, **36**, 3 (1965).
38. C. Jacinto, D. N. Messias, A. A. Andrade, S. M. Lima, M. L. Baesso, and T. Catunda, *J. Non-Cryst. Solids*, **352**, 3582 (2006).
39. R. A. Ganeev and A. I. Ryasnyansky, *Appl. Phys. B: Lasers Opt.*, **84**, 295 (2006).
40. D. D. Smith, Y. Yoon, R. W. Boyd, J. K. Campbell, L. A. Baker, and R. M. Crooks, *J. Appl. Phys.*, **86**, 6200 (1999).
41. R. F. Souza, M. A. R. C. Alencar, E. C. D. Silva, M. R. Meneghetti, and J. M. Hickmann, *Appl. Phys. Lett.*, **92**, 201902 (2008).